



## **AIAA 2002-0278**

# **Store Separation Simulation of Penguin Missile from Helicopters**

D. Lesieutre and M. Dillenius  
Nielsen Engineering & Research, Inc.  
Mountain View, CA

J.Gjestvang  
Kongsberg Defence & Aerospace AS  
Kongsberg, Norway

**40<sup>th</sup> AIAA Aerospace Sciences  
Meeting & Exhibit**  
**14-17 January 2002 / Reno, NV**

For permission to copy or republish, contact the copyright owner named on the first page.

For AIAA-held copyright, write to AIAA Permissions Department,  
1801 Alexander Bell Drive, Suite 500, Reston, VA, 20191-4344.

## STORE SEPARATION SIMULATION OF PENGUIN MISSILE FROM HELICOPTERS

Daniel J. Lesieutre<sup>\*</sup>, Marnix F. E. Dillenius<sup>†</sup>  
Nielsen Engineering & Research, Inc.  
Mountain View, CA

Jens A. Gjestvang<sup>‡</sup>  
Kongsberg Defence & Aerospace AS  
Kongsberg, Norway

### ABSTRACT

The store separation simulation code STRLNCH along with the intermediate-level missile aerodynamic prediction code MISDL has been adapted to model the launch and separation characteristics of the Kongsberg Defence & Aerospace (KDA) subsonic Penguin MK2 MOD7 missile configuration from a helicopter. The extensions of the Nielsen Engineering & Research (NEAR) STRLNCH simulation required the modeling of several characteristics unique to the Penguin. These include the Penguin aerodynamics and the dynamics associated with the folded and unfolding wings, the modeling of the wing unfolding inertial dynamics, the modeling of lanyard and lanyard release force effects, the characterization of wing roll tabs, the time-dependent thrust and mass properties, and the inclusion of a realistic autopilot. The modeling of the Penguin aerodynamics, including fully and partially folded wing effects, is handled with the NEAR MISDL/KDA aerodynamic prediction method which is described in detail in AIAA Paper 2002-0277. The resulting launch simulation method STRLNCH/KDA with MISDL/KDA was verified by comparing results to flight test data.

### LIST OF SYMBOLS

$l_R$	reference length
$C_l$	rolling moment coefficient
$M_\infty$	Mach number
$p, q, r$	rotational rates, roll, pitch, yaw
$x, y, z$	fuselage coordinate system; origin at the nose
$S_R$	reference area
$\alpha$	angle of attack, deg
$\alpha_c$	included angle of attack, deg
$\beta$	angle of sideslip, deg
$\delta$	canard deflection angle, deg
$\phi$	roll angle, deg
$\Psi, \Theta, \Phi$	Euler angles; yaw, pitch, roll

<sup>\*</sup> Senior Research Engineer, Senior Member AIAA

<sup>†</sup> President, Associate Fellow AIAA

<sup>‡</sup> Project Manager, Member AIAA

### BACKGROUND

The STRLNCH store separation simulation software is based on 1) modeling the flow field of a parent aircraft including fixed stores, 2) modeling the aerodynamics of the released store, and 3) integration of the six-degree-of-freedom equations of motion for the released store. Development of the NEAR store separation programs began in 1969 and was initially funded by the U.S. Air Force.<sup>2,3</sup> Since the initial development, the code has been enhanced under government (Air Force, Navy), commercial, and IR&D efforts.<sup>4,5</sup>

This paper describes the release of the Penguin missile from a helicopter, which includes several special modeling requirements. Figure 1 depicts a schematic of the helicopter with the Penguin missile in the carriage position. The modeling of the helicopter flow field and specific Penguin characteristics are described in this paper. Comparisons of predicted trajectories with flight test data and failure cases are presented. Modifications to the STRLNCH software required in this effort are described below.

### TECHNICAL DESCRIPTION

An overview of the modeling in the STRLNCH code and enhancements added to model specifics for the Penguin launch from a helicopter are given.

### GENERAL APPROACH

The STRLNCH subsonic store separation code<sup>5</sup> was used as the starting point in the development of the STRLNCH/KDA code for predicting trajectory characteristics of the Penguin missile released from a helicopter. The aircraft flow models are composed of module VTXCHN<sup>6</sup> for modeling the aircraft fuselage including vortex shedding and a vortex lattice for modeling both the wing/pylon and the interference shell for wing-on-fuselage aerodynamic interference.

The STRLNCH code is capable of modeling flow effects due to combined angle of pitch and sideslip as well as rotational rates of the parent aircraft. The store or missile aerodynamic loading calculation method was upgraded by using an enhanced version of the NEAR MISDL panel method-based missile aerodynamic prediction code.<sup>1</sup> This aerodynamic module provides the store aerodynamics for use in the STRLNCH 6-DOF trajectory calculations.

The flow models in the STRLNCH program are valid for subsonic Mach numbers (greater than zero) up to the critical speed or onset of transonic flow. The flow models represent effects of lift and thickness. Details of the horseshoe panel and other singularity-based flow models are described in References 2 through 5. Program STRLNCH includes first-order corrections to the wing horseshoe vortex panel method to account for high angle-of-attack effects. This includes a semi-empirical stall model to modify the wing horseshoe vortex panel strengths at high angles of attack.

A given fuselage and wing/pylon(s) combination is treated by solving first the fuselage alone and fixed stores (if any). A solution of the wing/pylon(s) and interference shell is then obtained with the fuselage and fixed store effects included in the flow tangency condition applied at the control points of the horseshoe vortex panels on the wing/pylon(s). In this way, the fuselage and fixed stores interfere on the wing/pylon(s), and the wing/pylon(s) interfere on the fuselage via the interference shell.

With the strengths of the singularities used to model the aircraft known, the flow field in the vicinity of any attached store is calculated. The parent aircraft perturbation velocities are then passed to the MISDL aerodynamic prediction method, and the store loads are calculated, including parent aircraft effects. The store is then moved to its next position under the influence of the calculated aerodynamic loads over a short integration time interval. The aerodynamic loads are recalculated and the store is moved to its next position. This process is repeated until the trajectory calculation is stopped.

### **MAJOR ENHANCEMENTS**

Enhancements made for KDA to the STRLNCH and MISDL codes to model the Penguin release from helicopters include the following:

1. helicopter rotor wake model,
2. hook release and hook delay model,
3. swaybrace forces and moments,

4. umbilical forces and moments,
5. Penguin autopilot model,
6. Penguin canard fin actuator model,
7. lanyard length model,
8. lanyard release model - release pin "pull-force,"
9. Penguin wing deployment dynamics model,
10. Penguin roll-tab rolling moment model,
11. rocket motor model,
12. time dependent mass and inertia properties,
13. automatic grid method for store loads in vicinity of carrier vehicle.

Further details of these enhancements follow. The resulting codes are designated STRLNCH/KDA and MISDL/KDA.

**Helicopter Rotor Wake Model.** The inclusion of a specified helicopter rotor wake model is an enhancement to the parent aircraft flow field model. Three methods for the user to specify the helicopter rotor wake have been implemented.

1. The simplest wake specifies a swept cylinder in which the wake downwash is constant. The center of the rotor wake, the wake radius, the sweep of the wake centerline, and a uniform downwash velocity are specified.
2. The second rotor wake input allows for a radial variation in downwash. The rotor wake geometry is a swept cylinder like the first option. However, the user can read in a downwash velocity that is a function of the radius from the hub to the tip of the rotor.
3. The third wake option is the most general and allows for an arbitrary wake to be specified which is a function of vertical, radial, and circumferential coordinates.

In any of the three methods, the mutual interference between the oncoming flow and the rotor wake is not accounted for.

**Hook Release and Hook Delay Model.** A hook release delay model is implemented. Two hooks can be modeled. One of the two hooks can be specified to release after a delay. The hook delay is formulated by enforcing the acceleration of the Penguin to be zero at the hook attachment point. The Penguin is free to drop/rotate subject to the constraint that the hook point is stationary. During the hook delay portion of the trajectory, there are three (3) additional state constraint equations which are integrated with the 6-DOF trajectory equations to ensure zero acceleration of the hook point. In addition, a hook breaking force can be

specified. If the hook constraining force exceeds the hook breaking force, the hook is released.

**Swaybrace Forces and Moments.** Based on swaybrace forces supplied by KDA, NEAR developed a two-degree-of-freedom model (vertical z position and angle from vertical  $\theta$ ) for the forces and moments. The swaybrace forces are assumed to act at a constant position and orientation on the Penguin, and are assumed to be a linear function of the two state variables z and  $\theta$ . The forces are assumed to act quickly (approx. 0.005 sec.), and aerodynamic forces are neglected. The equations of motion are integrated until the store falls clear of the last swaybrace. The change in states due to the swaybrace forces are used as initial conditions for the trajectory calculations.

**Umbilical Forces and Moments.** KDA specified the Penguin umbilical force versus vertical position. This umbilical has been modeled as an ejector in STRLNCH. The z-position is measured in a direction that is perpendicular to the missile centerline. When the missile is in carriage,  $z = 0$ . This functionality is included to investigate effects of failure of the Umbilical Retraction Unit (URU) in the bomb rack or of possible icing in the interface between the connector and the missile.

**Penguin Autopilot Model.** The Penguin autopilot subroutine used in the STRLNCH/KDA software is derived from the actual flight software. Changes have been made to exclude parts that are not related to the separation part of the flight and some simplifications have been introduced. The simplified routine has been compared to the full autopilot by using KDA's own simulation tools. The performance in the separation phase is for all practical purposes identical to the performance of the actual missile autopilot software. The autopilot consists of a PID controller with gain scheduling based on launch velocity and certain Euler angle considerations. The autopilot only controls azimuth and pitch since the missile is constantly rolling in flight due to fixed roll tabs on the wings. The simulation software allows for changes in the autopilot by compiling and linking the subroutine to the precompiled parts of the STRLNCH/KDA software.

The autopilot which commands canard fin control deflections is active prior to the release from the helicopter and is critical to modeling launch trajectory characteristics. For the launch phase, the autopilot logic commands deflections such that the initial heading of the Penguin is maintained.

**Penguin Actuator Model.** KDA supplied diagrams for a second-order actuator model including deflection angle, rate, and acceleration limiters. The actuator model was implemented in mathematical modeling software, and verified against KDA-supplied properties and step responses. A subroutine was written, verified and included in STRLNCH/KDA. The actuator model results in four (4) additional equations to be integrated with the standard 6-DOF equations for the launched store. There are two equations for the azimuth and two for the pitch channels of the autopilot. The input to the actuator model is the commanded deflections computed by the autopilot. The output is the actual fin deflections which are passed to MISDL/KDA to compute the aerodynamic forces at given instants of time during the trajectory calculation.

**Lanyard Length Model.** In order to determine when wing unfolding for deployment begins, a lanyard model is implemented. The lanyard for each Penguin wing is characterized by its attachment points to the helicopter and to the missile, and by its maximum deployed length. As part of the simulation, STRLNCH/KDA tracks the deployed length of each of the four (4) wing lanyards. When the maximum deployed length is reached, a release pin "pull-force" model is applied and wing deployment begins. For the flight test results presented (results section), a fifth lanyard is modeled associated with the Flight Termination System (FTS) system.

**Lanyard Release Model - Release Pin "pull-force."** During the pulling of the wing fold release pins, forces are applied to the Penguin through the lanyard. To model these forces, KDA supplied a specification of the force required to pull the pin. In STRLNCH/KDA it is assumed that: 1) the lanyard release event acts quickly, 2) the store orientation and mass are constant during the event, and 3) the lanyard forces and moments can be modeled as impulses.

$$\overline{F}_i = \int F_i dt$$

$$\overline{M}_i = \overline{F}_i x_i$$

The impulse model computes the change in translational and rotational velocities of the missile due to the pulling of each pin. These velocities are added as an increment to corresponding state variables for the store in the trajectory calculation.

**Penguin Wing Deployment Dynamics Model.** The unfolding mechanism of the Penguin wings consists of a spring and damper. The modeled dynamics of the Penguin wing deployment are based on a KDA Supplied Report.<sup>7</sup> The equations of motion for the wing

deployment angles and rates and the equations for the missile roll angle and rate (10 states) described in the referenced report were implemented in mathematical software for testing. These equations of motion include mass, inertia, deploying spring, and arresting damper terms. The results were verified against the KDA report, and a subroutine was written and verified.

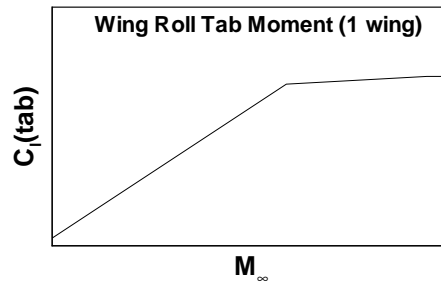
The wing deployment routine was considered for direct inclusion in the simulation equations of motion (as additional states). However, parametric studies performed with the deployment model indicated that the deployment of the wings is dominated by the spring and damper characteristics and that the missile states ( $\Phi$  and  $p$ , roll angle and roll rate) are only affected during the deployment. Conversely, the missile states ( $\Phi$  and  $p$ ) and aerodynamic effects only have a second- or higher-order effect on the wing deployment states (fold angle and unfolding rate). Additionally, the inclusion of the impulsive stopping of the wing deployment when the wing locks into place has the following effects: 1) the net imparted roll rate after deployment is 0.0, and 2) the net roll angle change after all 4 fins are deployed is nearly zero. It is not exactly zero because of the different fold angles.

Therefore, the modeling of the wing deployment dynamics through additional equations of motion in the simulation is not necessary or practical since the net effect on roll angle and roll rate is zero once all fins are deployed. For the simulation, the effects of each wing deploying on the missile roll angle, rate, and acceleration are stored in tabular format (versus time after deployment begins). These tables are read into the simulation. Table lookup is used for each wing individually and summed to get the overall effects on the missile states.

**Penguin Roll Tab Rolling Moment Model.** The Penguin wings have roll tabs which force the vehicle to roll. A direct method of modeling Penguin roll tabs is currently not implemented in MISDL/KDA.<sup>1</sup> This would require a panel layout which had panels specifically laid out on the roll tabs which could be deflected. To include the effects of roll tabs in the simulation, a Mach number dependent variation of wing roll tab rolling moment is read into the code. The KDA Low-Speed Wind Tunnel Data<sup>8</sup> does not provide a good model of the roll tab rolling moments. There is no Mach number effect and there is a variance between different tunnel tests.

Instead of the above, NEAR used the KDA Flight Test Data to formulate an empirical variation of tab rolling moment versus Mach number shown in the sketch

below. This provided the best agreement with the flight characteristics.



The empirical roll tab model is included as an input item for the MISDL/KDA aerodynamic module. For each fin, the individual characteristics of a roll tab can be specified, including: 1) the spanwise roll tab position, and 2) the roll tab moment as a function of Mach number. This allows individual fins to have different roll tabs and allows an approximation for the effect of the wing fold angle on the roll tab effectiveness.

**Rocket Motor Model.** KDA supplied thrust versus time tables for the Penguin booster and sustainer rocket motors. STRLNCH/KDA was modified to read in thrust time history tables for multiple rockets motors. An ignition time for each motor is also specified. During simulation the total thrust is the sum of all active motors.

**Time Dependent Mass and Inertia Properties.** KDA supplied the time dependent thrust and mass properties of the Penguin missile. Tables of time and mass,  $x_{cg}$ , and moments of inertia  $I_{XX}$ ,  $I_{YY}$ ,  $I_{ZZ}$ ,  $I_{XZ}$ ,  $I_{YZ}$ ,  $I_{XY}$  are read into STRLNCH/KDA. During the simulation, STRLNCH/KDA interpolates in the tables to determine mass and moments of inertia properties at any time.

**Automatic Grid Method for Store Loads.** STRLNCH/KDA was extended to perform store load calculations in the vicinity of the carrier vehicle at a user-specified set of grid field points and orientations. Two grid options are implemented:

1. **1. Traverse Grid Method:** this option allows the user to specify the store starting location  $(x,y,z)$  and orientation  $(\Psi, \Theta, \Phi)$  along with specified translations  $\Delta x$ ,  $\Delta y$ , and  $\Delta z$ . Loads are computed as the store is translated a specified number of times, but the orientation of store does not change.
2. **2. Grid Method:** the user inputs the number of grid points at which store loads are to be computed. STRLNCH/KDA reads the locations of each grid point, and the store's orientation  $(\Psi, \Theta, \Phi)$  at each grid point:  $(x, y, z)$ .

**Modeling of the Penguin Aerodynamics Including Folded-Wing Effects.** The MISDL software was modified to allow a spanwise fold line along the wing. In addition, the canard fin modeling was modified to allow the fins to conform to body nose shape. The modeling of the Penguin aerodynamics, including folded wing effects, is handled with the NEAR MISDL/KDA aerodynamic prediction method which is described in detail in AIAA Paper 2002-0277.<sup>1</sup> The modified code, MISDL/KDA, also includes effects of nonuniform flow. Figure 2 depicts MISDL panel layouts for the Penguin missile with wings folded and with wings deployed.

### **SELECTED RESULTS**

This section describes comparisons of predicted and flight test launch characteristics of the Penguin missile from a helicopter. Comparisons to data from two flight tests are given. In addition, a wing opening failure mode is investigated where two wings on one side fail to deploy. The Penguin missile in carriage on the helicopter is shown in Figure 1.

### **FLIGHT TEST DESCRIPTION**

The flight test telemetry data were collected in August 1994 in cooperation between KDA and one of KDA's customers. The test firings from the Sikorsky Seahawk helicopter were performed with production missiles where the warhead had been replaced by a telemetry unit and dummy masses to match the mass and inertias. More than 100 parameters were transmitted and available for analysis in addition to a number of conditions (flags) which change at least once during flight. All parameters from the inertial navigation platform were transmitted as well as the autopilot input and output. Most parameters were sampled at 50 Hz or higher. For the flight test results presented herein, vertical scale bars are included on the graphs which indicate the magnitude of the variable being plotted; specific values are not included on the vertical axes for KDA company proprietary reasons.

### **FLIGHT TEST 01**

For Flight Test 01, the angle of attack and sideslip of the helicopter at launch are each approximately 2°. Launch Mach number is low. For this forward flight speed, it is assumed that the rotor wake lies aft of the Penguin and therefore is not modeled. The autopilot is commanding a constant heading angle for the launch phase of the trajectory. The wing deployment and FTS lanyards are modeled. In the STRLNCH/KDA simulation, the outer wing lanyards pull at  $t \approx 0.415$  and the inner pair pulls at  $t \approx 0.485$ . The rocket motor

ignition in the simulations is at  $t = 0.75$ . Figure 3 presents the downrange and vertical position and velocities. There is good agreement between the predicted and flight test results. Figure 4 compares the Euler angles and the rotational rates. It is seen that the autopilot maintains the initial heading angle ( $\Psi$ ) and that the predicted roll characteristics are similar to flight test data. The effects of the wing unfolding dynamics can be seen in the roll rate ( $p$ ) graph, Figure 4(f). The magnitude and characteristic of the roll rate due to wing deployment matches the flight test but occurs slightly earlier. Figure 5 compares the Penguin angle of attack, angle of sideslip, commanded pitch and azimuth deflections, and the actual canard control deflections. These characteristics are hard to predict and to measure. Angle of attack and sideslip are usually estimated quantities in a flight test. Because of the autopilot, the predicted and measured deflections are expected to be different for several reasons: 1) the flight test and predicted aerodynamics may not agree exactly for all times, 2) the parent aircraft flow model may not be exactly that of the actual helicopter, and 3) there may have been winds present not modeled in the simulation. Errors in any of these models will cause the autopilot to produce different deflections. However, the autopilot in both cases is working correctly as indicated in Figures 3 and 4. The vertical position is in good agreement, Figure 3(c) and the heading angle is maintained, Figure 4(a).

### **FLIGHT TEST 02**

For Flight Test 02, the angle of attack is approximately 2° and the angle of sideslip is approximately 6° at launch. Figures 6, 7, and 8 depict the results for these launch conditions. The results are similar to Flight Test 01. The predicted and measured position and velocity are in good agreement, Figure 6; the heading angle ( $\Psi$ ) is maintained by the autopilot, Figure 7(a); and the roll characteristics are predicted well, Figure 7(c and f). Because of the higher sideslip angle at launch, large azimuth deflections are commanded to maintain heading, Figure 8(e). Figure 8(f) indicates that one set of fins has reached the deflection limit of the actuator (at least in the prediction). However, this does not limit the ability of the Penguin to have a successful launch and trajectory.

### **WING DEPLOYMENT FAILURE ANALYSIS**

An examination of a wing opening failure mode is presented. The failure mode modeled involves failure of one of the outer Penguin wings (outboard) to deploy. This forces both outboard wings to remain folded, see Figure 1. The launch conditions for this investigation

are the same as for Flight Test 01. Results of the failure mode are plotted with Flight Test 01 results in Figures 9 and 10. From time 0 to 3 secs., very little difference is seen in the position and velocity results, Figure 9. However, for  $t$  greater than 3, the wing failure results indicate higher vertical upwards velocity than the Flight Test 01 case, Figure 9(d). Figure 10(a) indicates that the autopilot is still able to maintain the initial heading angle,  $\Psi$ . The primary effect of the wing failure is on the roll characteristics, Figure 10(b and c). With one set of wings folded, the roll tabs are not able to spin the missile, Figure 10(c), and the Penguin rolls to a nearly “static” orientation where the deployed wings are essentially in a “V-tail” orientation, Figure 10(b). To reach this nearly static orientation, there is a large damped oscillation in roll with rates approaching 300 deg/s.

### CONCLUSIONS

The store separation simulation code STRLNCH along with the intermediate-level missile aerodynamic prediction code MISDL have been adapted to model the launch and separation characteristics of the Kongsberg Defence & Aerospace (KDA) subsonic Penguin missile configuration from a helicopter. The extensions to the STRLNCH simulation required the modeling of several characteristics unique to the Penguin. The paper describes how the resulting STRLNCH/KDA code handles the Penguin aerodynamics and the dynamics associated with the folded and unfolding wings, the wing unfolding inertial dynamics, the lanyard and lanyard release force effects, the wing roll tabs, the time-dependent thrust and mass properties, and the realistic autopilot. Overall, the STRLNCH/KDA simulation with MISDL/KDA predicts launch characteristics of the Penguin that agree well with flight test telemetry data. The simulation also allows for launch failure studies such as wing deployment failure and hook release delays.

### ACKNOWLEDGMENT

The work reported herein was performed under contract to Kongsberg Defence & Aerospace (KDA) by Nielsen Engineering & Research (NEAR). The cognizant engineers at KDA are Mr. Jens A. Gjestvang and Mr. Helge Morsund.

### REFERENCES

1. Lesieutre, D. J., Dillenius, M. F. E., and Gjestvang, J. A., “Application of the MISDL/KDA Aerodynamics Prediction Method to Penguin Missile,” AIAA 2002-0277, Jan. 2002.
2. Goodwin, F. K., Dillenius, M. F. E., and Nielsen, J. N., “Extension of the Method of Predicting Six-Degree-of-Freedom Store Separation Trajectories at Speeds up to Critical Speed, Vol. I, Theoretical Methods and Comparison with Experiment,” AFFDL-TR-72-83, 1972.
3. Goodwin, F. K., Dillenius, M. F. E., and Nielsen, J. N., “Extension of the Method of Predicting Six-Degree-of-Freedom Store Separation Trajectories at Speeds up to Critical Speed to include a Fuselage with Non-Circular Cross Section,” AFFDL-TR-74-130, Vol. I, 1974.
4. Dillenius, M. F. E., Lesieutre, T. O., and Lesieutre, D. J., “Subsonic Parent Aircraft Flow Prediction Program SBPAFL,” NEAR TR 485, Dec. 1994.
5. Dillenius, M. F. E., Love, J. F., Hegedus, M. C., and Lesieutre, D. J., “Program STRLNCH For Simulating Missile Launch From A Maneuvering Parent Aircraft At Subsonic Speed,” NEAR TR 509, Sep. 1996.
6. Hegedus, M., Dillenius, M. F. E., and Love, J., “VTXCHN: Prediction Method For Subsonic Aerodynamics and Vortex Formation on Smooth and Chined Forebodies at High Alpha,” AIAA 97-0041, Jan. 1997.
7. “Penguin MK2 MOD7 Wing Deployment Analysis,” Kongsberg Defence Products Division, Document No. FP207-UHK-22-0436, Mar. 1985.
8. “Penguin MK2 MOD7 Low Speed Wind Tunnel Test Report,” Kongsberg Defence & Aerospace AS., Document No. 01TR68072909, Jan. 1998.

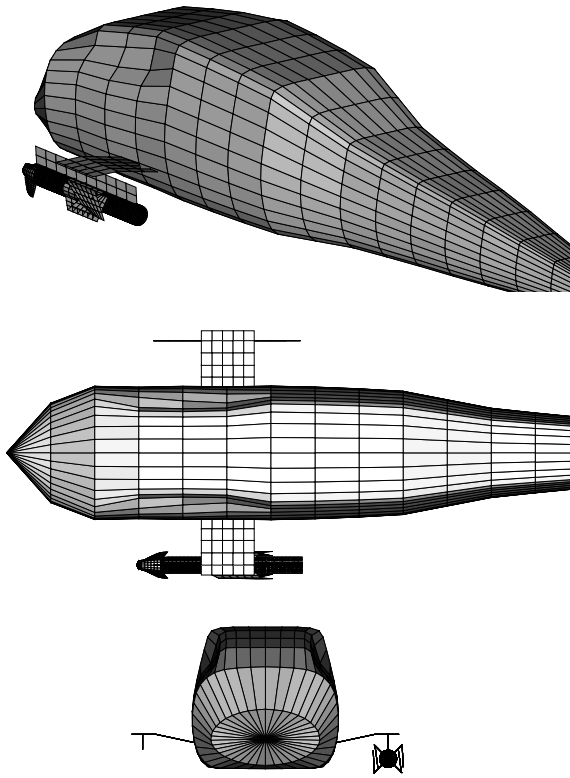


Figure 1.- Schematic of helicopter with Penguin missile in carriage position.

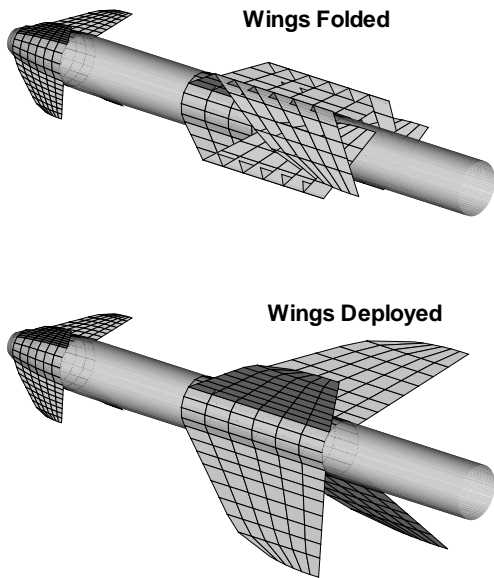


Figure 2.- MISDL/KDA panel layout for wings folded and wings deployed configurations.

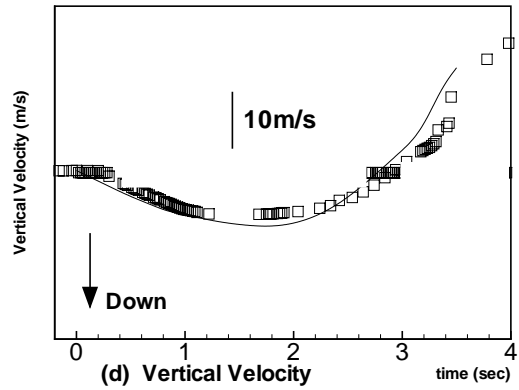
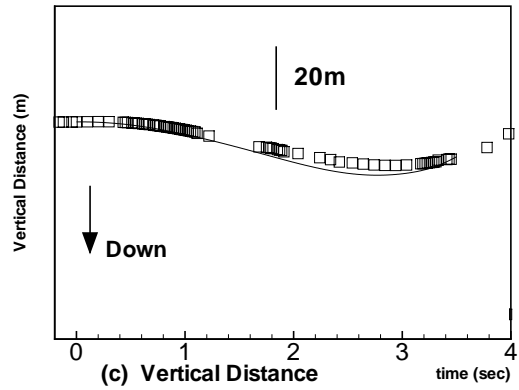
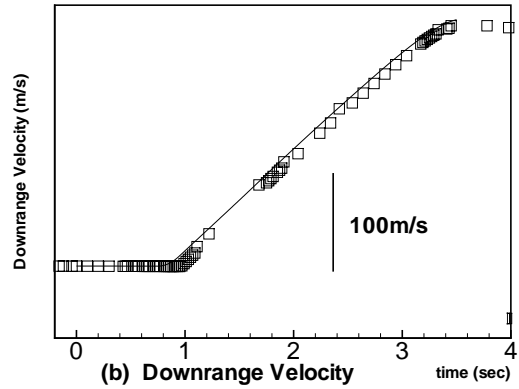
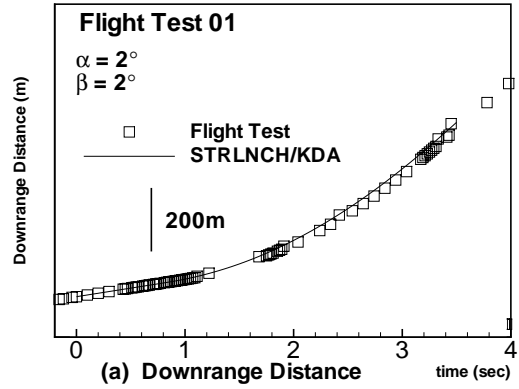


Figure 3.- Comparison of predicted and flight test position and velocity for Flight Test 01.



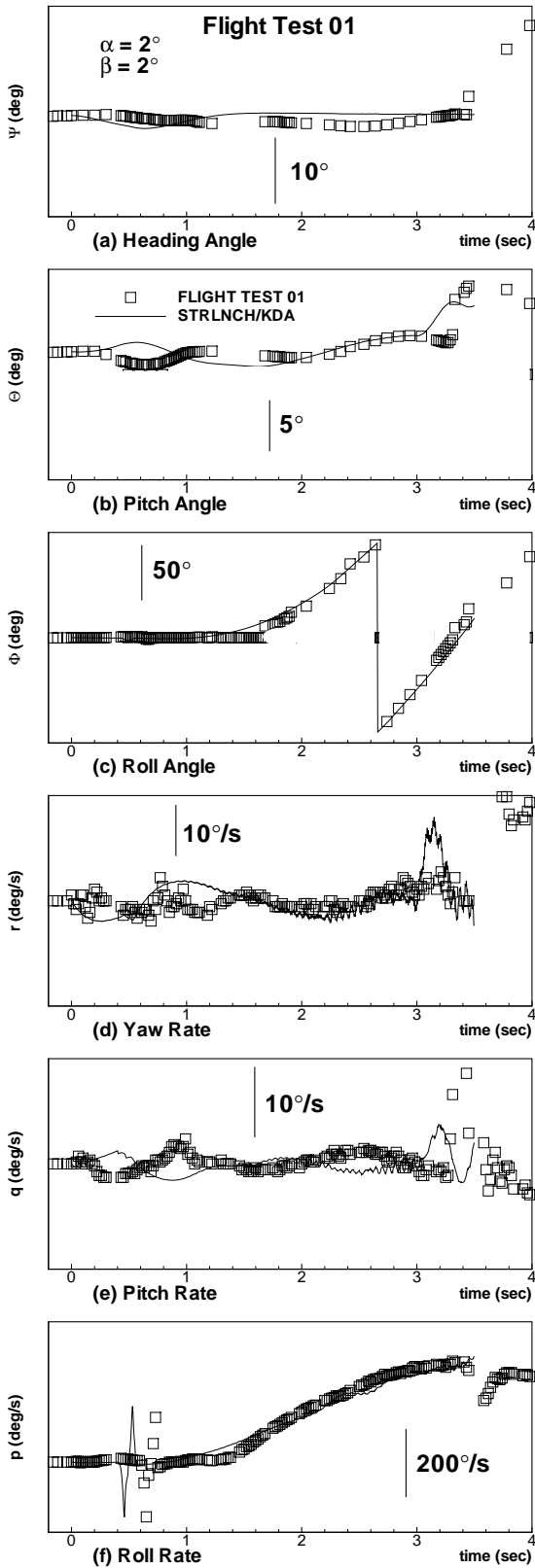


Figure 4.- Comparison of predicted and flight test Euler angles and rotational rates for Flight Test 01.

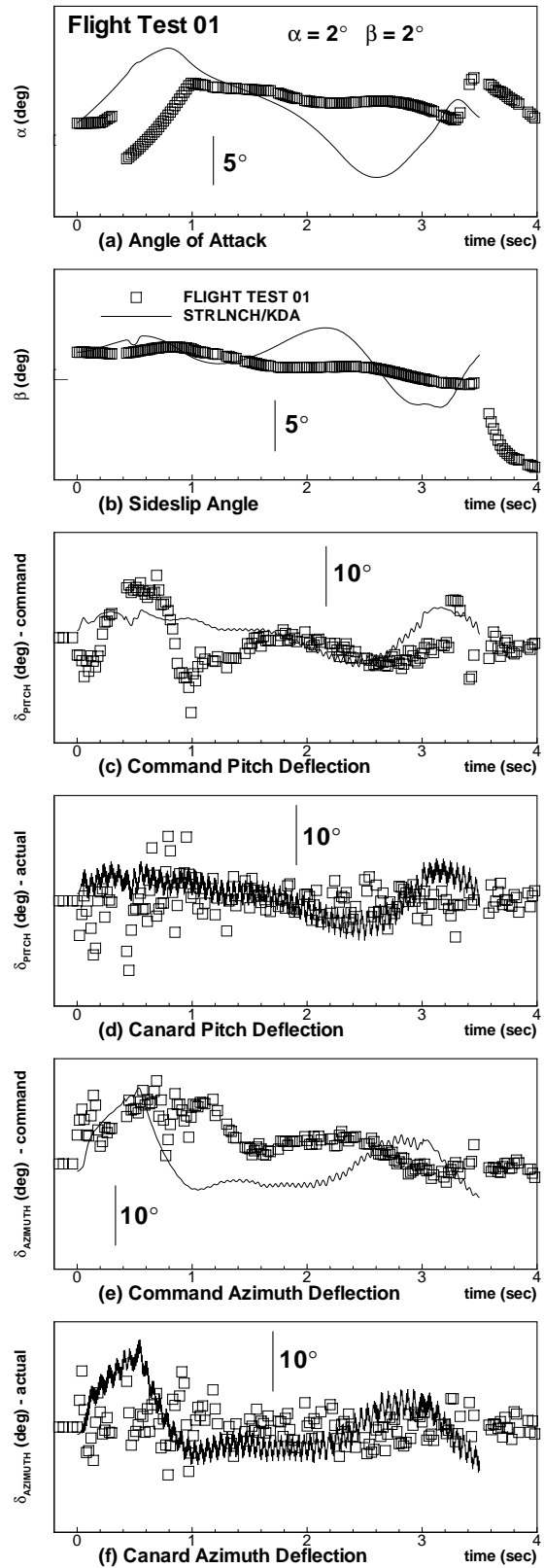


Figure 5.- Comparison of predicted and flight test flow angles and deflection angles for Flight Test 01.

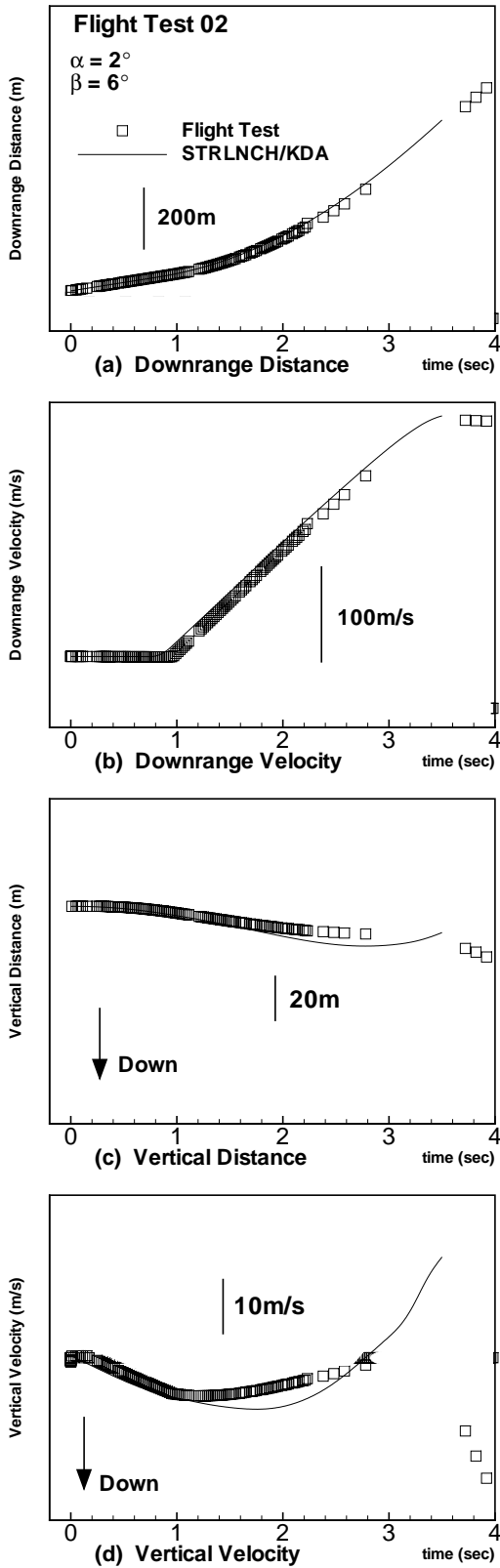


Figure 6.- Comparison of predicted and flight test position and velocity for Flight Test 02.

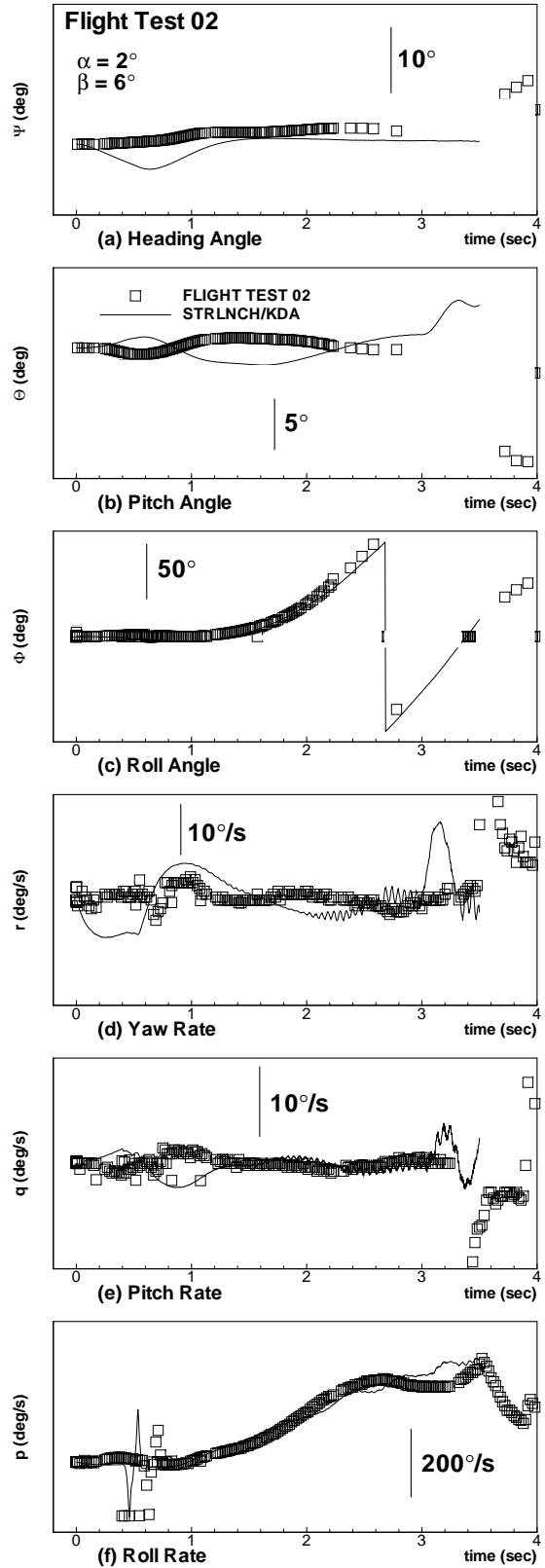


Figure 7.- Comparison of predicted and flight test Euler angles and rotational rates for Flight Test 02.

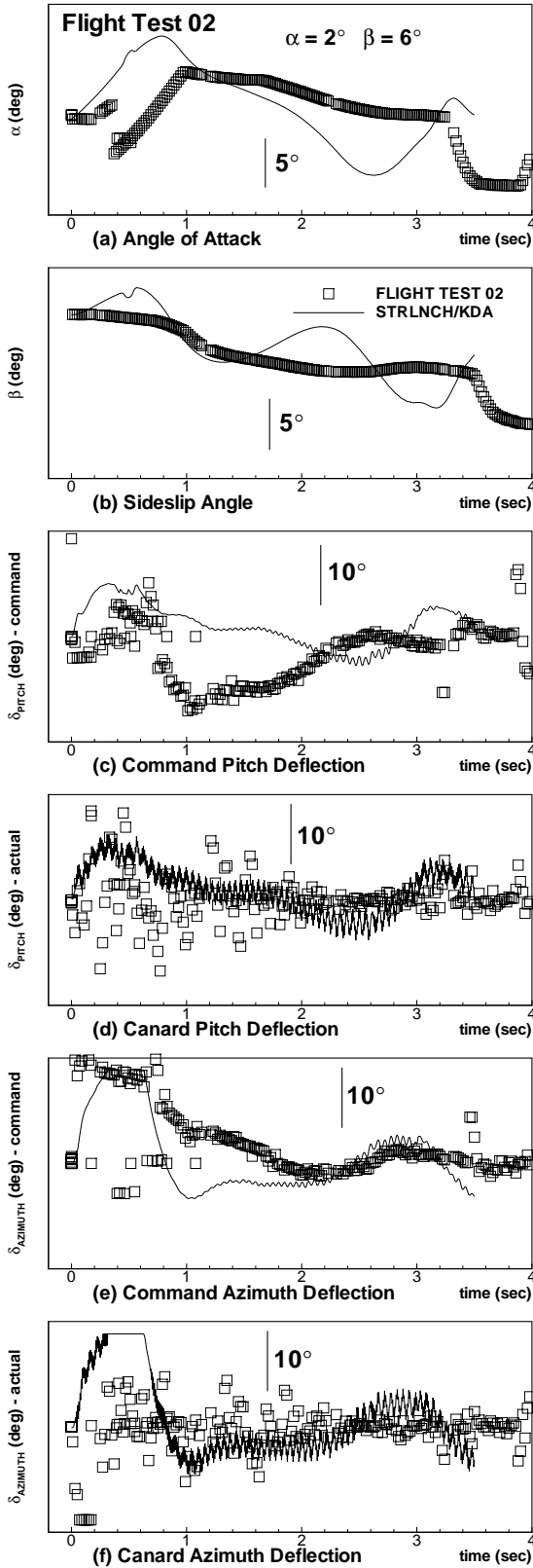


Figure 8.- Comparison of predicted and flight test flow angles and deflection angles for Flight Test 02.

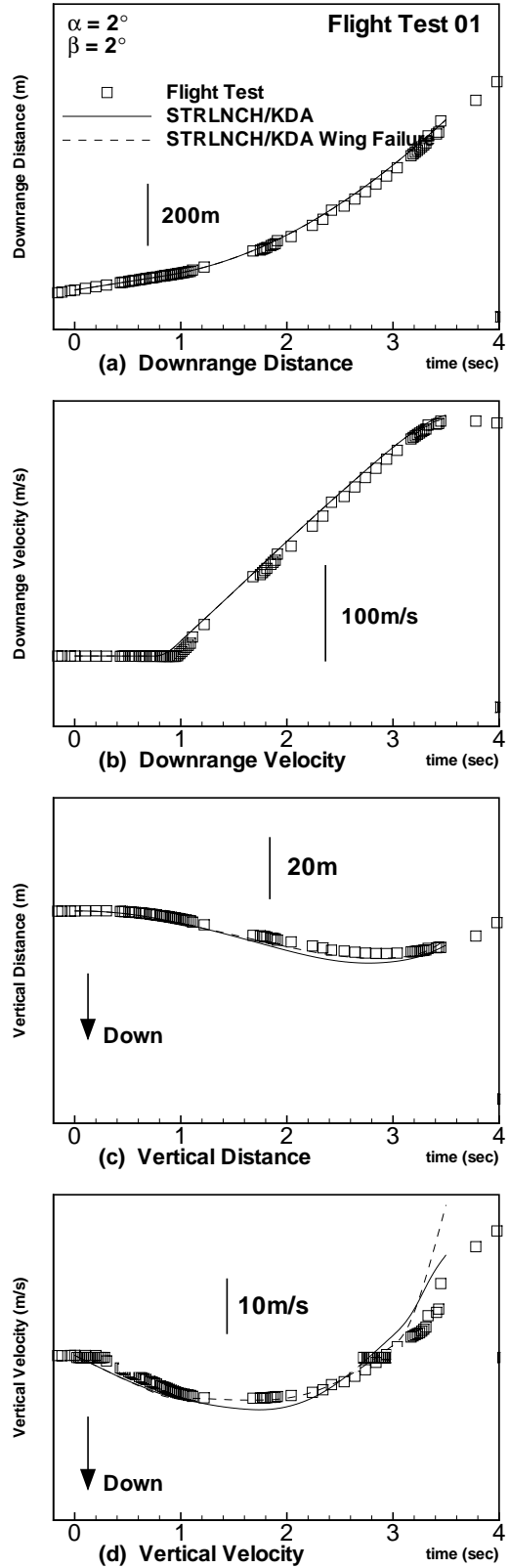


Figure 9.- Comparison of nominal and wing opening failure for Flight Test 01 launch conditions; position and velocity.

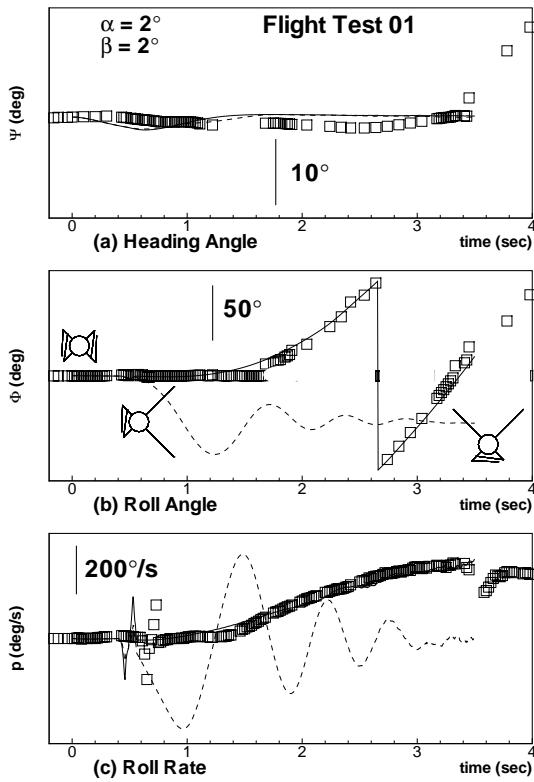


Figure 10.- Comparison of nominal and wing opening failure for Flight Test 01 launch conditions; Euler angles and rotational rates.